International Journal of Adhesion & Adhesives 34 (2012) 107–116

Contents lists available at SciVerse ScienceDirect

International Journal of Adhesion & Adhesives

journal homepage: www.elsevier.com/locate/ijadhadh

Adhesive properties of acrylate copolymers: Effect of the nature of the substrate and copolymer functionality

Yana Peykova [a], Olga V. Lebedeva [a], Alexander Diethert [b], Peter Müller-Buschbaum [b], Norbert Willenbacher [a,*]

[a] Karlsruher Institut für Technologie (KIT), Institut für Mechanische Verfahrenstechnik und Mechanik, Gotthard-Franz-Straße 3, 76131 Karlsruhe, Germany
[b] Technische Universität München, Physik-Department, Lehrstuhl für Funktionelle Materialien, James-Franck-Straße 1, 85748 Garching, Germany

ARTICLE INFO

Article history:
Accepted 28 November 2011
Available online 8 December 2011

Keywords:
Pressure-sensitive
Rheology
Tack
Viscoelasticity
Acrylate copolymers

ABSTRACT

The adhesion behavior of statistical, uncrosslinked butyl acrylate-methyl acrylate copolymer on different surfaces (stainless steel, polyethylene, glass and Si-wafer) has been investigated using a combination of probe tack test and simultaneous video-optical imaging. Tack and stress peak values increase and the final number of cavities as well as cavity growth rate decreases with increasing surface energy of the substrate due to better wetting.

The influence of the incorporation of an additional comonomer, namely, hydroxyethyl acrylate, methyl methacrylate and acrylic acid, on the adhesion of statistical, uncrosslinked butyl acrylate-methyl acrylate copolymer has been studied. Steel probes with different average surface roughness (R_a = 2.9 and 291.7 nm) have been used for tack tests. The increasing polarity of the incorporated comonomer has no measurable effect on the surface tension but leads to an increase of shear modulus and consequently, to an increase in the stress peak, deformation at break, tack values, as well as the total number of cavities. The latter is a consequence of worse wetting. Cavity growth rate on the smooth surface is insensitive to copolymer composition, on the rough surface, the increase in the modulus associated with the additional monomers, leads to a decrease in the cavity growth rate. This indicates different cavity growth mechanisms: predominately lateral growth on the smooth surface and omnidirectional growth on the rough surface.

The adhesion performance of uncrosslinked and crosslinked butyl acrylate-methyl acrylate copolymers is compared. The latter exhibit adhesive, and the former cohesive failure. The total number of cavities and cavity growth rate is found to be controlled by viscoelastic properties of PSA independent of the debonding mechanism and the latter decreases significantly with increasing shear modulus.

© 2011 Elsevier Ltd. All rights reserved.

1. Introduction

The adhesion performance of pressure sensitive adhesives (PSAs) is determined by three properties: tack, peel strength (adhesion) and shear strength (cohesion). Tack is a dominant property of PSAs and is defined as the ability to adhere to any surface under low (1–10 Pa) contact pressure and short (1–5 s) contact time without any change in temperature or chemical reaction [1]. The probe tack test with a flat-end cylindrical probe [2,3] is widely used to test short-time and low-pressure adhesion. The advantage of this test is that the adhesive film is exposed to a uniform stress and strain rate over the whole surface of the probe. Additionally, microscopic analysis of the sequence of events occurring during the tack test is necessary to attempt a detailed interpretation of a tack curve and to better understand the debonding mechanism.

The parameters, which influence the results of the probe tack tests and consequently the adhesion of PSAs can be divided into three groups. First, the experimental parameters of the tack test such as temperature, contact time and contact pressure can be varied in the probe tack test and these parameters can considerably change the fracture mechanism [4,5].

Secondly, the properties of the probe used in the tack test such as probe (adherent) material and its surface roughness also strongly influence the adhesion of PSAs. The effect of surface roughness was discussed in several earlier studies [6–8] and in our previous work [9] we have presented a detailed investigation of the effect of surface roughness of a steel substrate on the adhesion of uncrosslinked acrylate copolymers and have shown that surface roughness strongly influences the work of adhesion

* Corresponding author.
E-mail address: norbert.willenbacher@kit.edu (N. Willenbacher).

0143-7496/$ - see front matter © 2011 Elsevier Ltd. All rights reserved.
doi:10.1016/j.ijadhadh.2011.12.001

as well as size and number of the cavities, however the cavity growth rate is found to be insensitive to surface roughness, but strongly controlled by viscoelastic properties of PSA. Some earlier studies [3,10–12] and several recent studies [13–17] are related to the investigation of the effect of surface energy of the substrate (i.e. probe in the tack experiment) on the adhesion of PSAs. In [10,11] it was shown that maximum tack and cavitation is achieved with adherents whose surface tension is slightly higher than that of the adhesive. Good wetting of the adherent by the adhesive is also very important for high tack, which is fulfilled if the adherent has a higher surface tension than the adhesive [3]. In the recent studies [13–17], the influence of the composition of PSAs on their adhesive performance on the low-energy surfaces has been studied and synthesis of PSAs with good adhesion on low-energy surfaces has been attempted.

Thirdly, the molecular parameters of an adhesive, such as glass transition temperature, molecular weight, polydispersity, monomer composition and degree of crosslinking are responsible for the adhesion behavior of PSAs [2]. The influence of these parameters have been studied in considerable detail [9,18–23]. But the interpretation of the results is often not trivial, because changing e.g. of monomer composition generally leads to changes in gel fraction or molecular weight distribution, and consequently changes in particular the viscoscoelastic properties of the PSA [22,23]. Furthermore, changes of the monomer composition often change both the bulk and surface properties and accordingly the adhesion performance of PSA. In an earlier study [24] there was an attempt to separate the bulk and interfacial effects of acrylic acid on the adhesion of poly(*n*-butyl acrylate) (PnBA). It was shown that the presence of 10% by weight of acrylic acid in the polymer appears to increase the thermodynamic work of adhesion by a factor of about 1.5. The change in viscoelastic properties of the adhesive bulk also increases the peel force.

Some early studies are related to the effect of comonomer composition and polarity on the adhesion performance of PSAs [20,22,23,25–27]. Incorporating a small amount of polar comonomer (AA), methacrylic acid (MAA), hydroxyethyl acrylate (HEA) and acrylonitrile (AN) increases the tack [25]. Acid groups have the greatest effect, and tack reaches its maximal value at 3–4 mol% incorporation of either AA or MAA. The authors explain this variation in terms of competition between improved interfacial bonding due to the polar groups and a decrease in deformation ability due to the strong increase in shear modulus with increasing content of acid groups. In [22] the effect of varied monomer composition on adhesion of acrylate copolymer with constant T_g and AA content was studied and it was shown that the tack was constant through all compositions. In this case tack seems to be determined by T_g or softness of the copolymers, and the constant polar AA concentration. Another experimental study [26] revealed that incorporating AA in PnBA leads to an increase in relaxation times of the polymer and to a significant increase in adhesion to glass substrates. In [20] it was shown that AA groups have a substantial effect on the large-strain extensional properties of PnBA and cause a shift in the characteristic debonding rate at which the transition from cohesive to adhesive failure is observed. A systematic study on adhesive and rheological properties as well as the debonding mechanism of slightly crosslinked acrylic networks based on EHA [27] showed that the addition of a polar comonomer (AA) increases both, the elastic modulus and the resistance to interfacial crack propagation. The increase of the latter with increasing AA content is the dominant effect at low debonding rates/high temperatures whereas the increase of the elastic modulus with increasing AA content becomes dominant at high rates/low temperatures.

As already mentioned above, adhesion is strongly affected by the degree of crosslinking of the polymer, due to its effect on the viscoelastic properties of the polymer. The adhesive performance of crosslinkable PSAs can be varied in a wide range, more densely crosslinked PSAs show cohesive behavior while slightly crosslinked PSAs are tacky [28,29]. One of the most preferable methods recently introduced for crosslinking of PSA films is UV technology; the advantage is that degree of crosslinking and the adhesion-to-cohesion ratio of PSAs can be varied by controlling the UV dose and this makes it possible to manufacture a wide range of adhesives with different properties from a single raw material. Adhesive failure is observed at high, and cohesive fracture at low UV dose. Tack shows a maximum near the gel point ($G' \approx G''$ over a broad frequency range) [29]. Similar results were obtained for model polydimethylsiloxane (PDMS) model systems [30]. Experiments with PnBA films, UV crosslinked to different degrees beyond the gel point [31], show that with increasing crosslinks density deformation at break decreases while stress peak and the height of the plateau remain more or less constant. The adhesion performance of UV-crosslinkable PSAs was studied in [32,33]. The authors used high UV dose and as a result tack and peel resistance were significantly reduced.

The goal of this study is threefold. First, we study the adhesion of statistical, uncrosslinked butyl acrylate-methyl acrylate copolymers on different surfaces. Second, we incorporate additional comonomer, namely, hydroxyethyl acrylate, methyl methacrylate and acrylic acid, and study its influence on the adhesion of the butyl acrylate-methyl acrylate copolymer. Third, we study the influence of crosslinking on the adhesion and debonding mechanism of butyl acrylate-methyl acrylate copolymer. In our study, we use the probe tack test in a combination with a simultaneous video-image analysis. Our experimental set-up allows for observation of the debonding process and corresponding cavity formation in situ with high spatial and temporal resolution, images of the contact area of the probe with the PSA film are simultaneously recorded with the contact force at every stage of the tack test. The quality of the obtained images enables us to obtain reliable results for the number and size of cavities formed. This also allows for a study of the kinetics of cavitation in detail and to evaluate the cavity growth rate.

2. Experimental

2.1. Materials

The PSAs used in this study were model statistical acrylic copolymers with different composition, characteristic features are shown in Table 1.

The model copolymers p(nBA-stat-MA), p(nBA-stat-MA-stat-HEA), p(nBA-stat-MA-stat-MMA) and p(nBA-stat-MA-stat-AA) were synthesized via radical solution polymerization in a semi-batch

Table 1
Model copolymers.

Composition	Ratio[a]	M_w (g/mol)	M_w/M_n	Supplied as
BA/MA	79.7/20	54,000	3.9	71% solution in MEK
BA/MA	79.7/20	192,000	6.4	80% solution in MEK
BA/MA	79.7/20	600,000	13.6	49.4% solution in n-butyl-acetate
BA/MA/HEA	79.7/15/5	193,000	6.7	80.6% solution in MEK
BA/MA/MMA	79.7/10/10	195,000	7.0	65% solution in MEK
BA/MA/AA	79.7/15/5	191,000	7.1	80% solution in MEK

BA=butyl acrylate, MA=methyl acrylate, AA=acrylic acid, MMA=methyl methacrylate, HEA=hydroxyethyl acrylate, MEK=methyl ethylketone.

[a] All copolymers contained 0.3% of photoinitiator.

procedure at 80 °C in MEK (low and intermediate molecular weight samples) or in n-butyl-acetate (high molecular weight sample) and 80% solids-content with a peroxide starter.

Transparent glass slides ($200 \times 50 \times 3$ mm) were purchased from Hera Glas GmbH, Germany. Abrasive papers were purchased from Bühler GmbH, Germany. Acetone was purchased from Carl Roth GmbH+Co. KG, Germany. The probes used for the tack measurements were flat-ended cylinders with a diameter of 5 mm made of stainless steel, type 1.4034 (Eisen Schmitt GmbH & Co. KG, Germany), glass (Hera Glas GmbH, Germany), transparent low density polyethylene LD-PE (Fritz Bossert, Germany) and silicon Si-Wafer (SiTec, Germany).

2.2. Methods

2.2.1. Rheological measurements

Rheological measurements were performed on a rotational rheometer RS-150 (ThermoHaake GmbH, Germany) using cone and plate fixtures (cone diameter: 20 mm; cone-angle: 1°).

2.2.2. PSA films preparation and characterization

For our experiments we used 50 ± 5 μm thick adhesive films prepared by coating the PSA solutions onto clean glass slides using a home-made doctor blade with a gap in combination with an automatic film applicator coater ZAA 2300 (Zehntner GmbH, Switzerland). The coating speed used for the film preparation was 20 mm/s. Freshly prepared films were stored at room temperature overnight (for at least 12 h) to allow slow solvent evaporation without bubble formation, and subsequently at 120 °C for 1.5 h to evaporate the remaining solvent and to get a smoother polymer surface.

The PSA film thickness was determined by two independent methods. According to the first method the film thickness was measured by a dial gauge with a flat-ended feeler using silicon paper to avoid adhesion between the feeler and the film. Alternatively, the film thickness was determined from a force-distance curve obtained from a tack measurement. The distance was calibrated to zero at the surface of the glass substrate. The difference between the known substrate position and the position, at which the first contact with polymer material takes place, i.e. the position at which the first negative force value is detected, gives information about the film thickness. Both methods provided similar results.

The composition of the PSA films was studied using X-ray reflectivity [34]. The measurements were performed using a Siemens D5000 Diffractometer (Siemens AG, Germany) according to the method described in detail in Ref. [35].

The UV-crosslinked samples were prepared using the following procedure. BA/MA films deposited onto the glass slides were cured using a UV lamp (UV-Handlampe NU-15 KL, Benda, Germany) with an intensity of 1.45 mW/cm^2 measured at a distance of 4.5 cm and wavelength of 254 nm. The exposure times used were 0, 21, 28, 34 and 69 s corresponding to the UV doses 0, 30, 40, 50 and 100 mJ/cm^2, respectively; according to the intensity of the lamp given above.

2.2.3. Probe preparation and characterization

The probes used for tack experiments were prepared from stainless steel, polyethylene (PE), glass and Si-wafer. To prepare stainless steel probes with various average surface roughness (R_a=2.9, 41.2 and 291.7 nm) flat-ended cylinders of stainless steel were polished to different degrees with abrasive papers and with a diamond dispersion (diameter of particles 1 μm). For the preparation of the PE probe (R_a=49.5 nm), a transparent foil of low density PE was glued onto a Si-wafer to ensure high quality imaging of the cavitation process. To prepare glass probes (R_a=2.36 nm) two transparent glass cylinders were cut using ultrasonic cutting. The glass probe was soaked for an hour in aceton to clean the surface from eventual polymer rest or dust and after that was hydrophobized using trimethylclorosilane TMCS [36,37]. To get a contact angle of 100° with distilled water, similar to the one on PE, we used 100% TMCS. To prepare Si-wafer probe (R_a=1.6 nm), a Si-wafer cylinder was cut using ultrasonic cutting. The diameter of all probes was 5 mm and the R_a of the probe surface was measured using a Q-Scope™ Scanning Probe Microscope (SPM) (Ambios Technology, Inc., USA) as described before [9].

2.2.4. Contact angle measurements and determination of the surface energy of copolymers and probes

Contact angles were measured according to the sessile drop method using Contact Angle System OCA (DataPhysics Instruments GmbH). The test liquids used were distilled water, ethylene glycol, diiodomethane and paraffin oil. The values of the contact angles of the test liquids with different probes and copolymer films were recorded as a function of time. The images were recorded automatically for 60 s at a rate of 10 frames/s. After extrapolating the curves we get for the contact angle vs. time, the value for the contact angle was ascertained as the stready state value avaraged from 6 experiments. Surface energy values were calculated from the measured contact angles according to the method of Owens and Wendt described in [38].

2.2.5. Tack experiment and video-optical observation

The experimental set-up used for the tack measurements and video-optical observation was described before [9]. Briefly, the set-up is based on the commercial device Texture Analyzer TA.XTplus (Stable Micro Systems, UK) with a measured compliance of 2.75 μm/N and modified with a quartz force sensor (Kistler Instrumente GmbH, Germany) that has a force range ± 500 N and a threshold of 1 mN. The glass slide with the deposited PSA film is positioned on the home-built vacuum table. The probe tack tests were performed as follows: the probe approached the sample with a rate 0.1 mm/s, contacted the adhesive film with a contact force of 10 N and was held at a constant position for 1 s. The probe was then withdrawn with a constant rate of 0.1 mm/s. The resulting force-distance curves were recorded simultaneously with video images of the contact area. Testing was performed at a temperature of 22 °C. The surface of the probe was cleaned with acetone before each test. To get reliable average values each sample was tested at least 5 times.

From the stress vs. strain curves obtained in tack experiments, the stress peak σ_p and the deformation at break ε_B were determined. The measured force F was converted to a nominal stress $\sigma = F/A_0$, where A_0 is a true initial contact area, measured from the optical images, taken at the beginning of the pull-off stage. The tack value was obtained from the area under the nominal stress vs. nominal deformation (strain) curve. The latter was calculated from the time-dependent film thickness h as $\varepsilon = (h - h_0)/h_0$, where h_0 is the initial film thickness.

The video images were obtained with a high-speed camera KL MB-Kit 1M1 (Mikrotron GmbH, Germany) used in combination with a zoom objective 90° KL-Z6 and a cold light source KL3000B. The camera allows to record 124 frames/s at maximum resolution of 1280×1024 pixels (1 pixel is approx. 5 μm).

The force-time curve was synchronized with the video sequence in such a way that the first contact of the probe with the sample in the force curve corresponds to the image showing the first contact (the first image recorded corresponds to the

moment when it was observed that the probe touches the surface of the polymer film). The videos were quantitatively analyzed using Visiometrics Image Processing System software (Prof. Dr. Stephan Neser, University Darmstadt). The true contact area and growth rate of individual cavities were determined.

3. Results and discussion

3.1. Influence of the material of the probe on the adhesion of BA/MA PSAs

Fig. 1 shows the values of the parameters calculated from stress–strain curves, i.e. stress peak, deformation at break and tack for BA/MA PSA measured with probes of different materials. We were not able to prepare a smooth PE probe ($R_a \ll 50$ nm) in such way that one can obtain high quality images of the contact area. Therefore, a PE probe with $R_a = 49.5$ nm was prepared and used for the tack tests. But it should be kept in mind, that surface roughness had a significant effect on cavitation [9]. Accordingly, we give the values calculated from the stress–strain curves for steel probes with $R_a = 2.9$ and 41.2 nm, so that one can compare values for steel and PE probe with $R_a \sim 45$ nm. Additionally, we hydrophobized a glass probe with $R_a = 2.4$ nm and obtained contact angle and surface energy values similar to PE. Thus, one can compare values for steel, glass and hydrophobic glass (similar to PE properties) with $R_a \sim 2$ nm. Surface energies of all substrate used in this study were calculated via contact angle measurement and have followed values: γ(hydrophilic glass) $= 68 \pm 4.8$ mJ/m^2; γ(hydrophobic glass) $= 26 \pm 4.1$ mJ/m^2; γ(steel) $= 43 \pm 4.7$ mJ/m^2; γ(PE) $= 30 \pm 1.5$ mJ/m^2; γ(Si-wafer) $= 64 \pm 5.6$ mJ/m^2.

The tack curves measured with glass and Si-wafer probes show the highest stress peak and tack values corresponding to the lowest contact angle and highest surface energy values. The most hydrophobic surfaces, PE and hydrophobic glass, show the lowest stress peak and tack values. The deformation at break is independent of the probe material, as expected, since it is mainly controlled by the viscoelastic properties of the polymer material and surface nature plays no role. In agreement with earlier studies [3,7] stress peak and tack values decrease with decreasing surface energy on the substrate, whereas the maximum work of adhesion reported in [10,11] was measured on a substrates with values of surface energy near to the value of the polymer film.

The images of the contact area PSA/probe were also recorded and the cavitation process was studied. As in our previous work [9] two types of cavities were observed. The cavities of the first type appear at the very beginning, long before the stress approaches its maximum. These cavities grow slowly from the beginning of debonding and then increase their growth rate when the stress peak is approached. The second type cavities appears at the area of the stress maximum and grow with higher rate. The final number of cavities is shown in Fig. 2 together with corresponding images of the contact area. The number of cavities decreases and, accordingly, their size increases with increasing surface energy of the substrate due to better wetting. In the case of hydrophilic probes, no additional cavities appear after the stress peak is reached; however, some additional cavities appear even after the maximum of the stress peak is passed on the

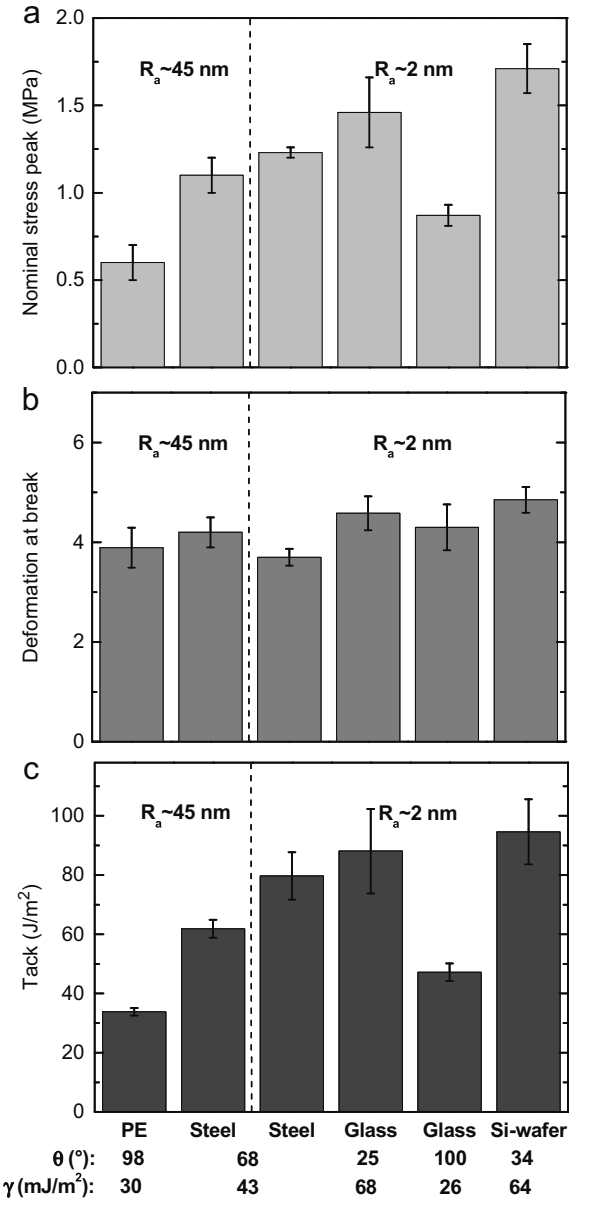

Fig. 1. Stress peak (a), deformation at break (b) and tack (c) for the probes of different materials measured using BA/MA ($M_w = 192{,}000$ g/mol) as PSA. Contact angle probe/water and surface energy values are also given.

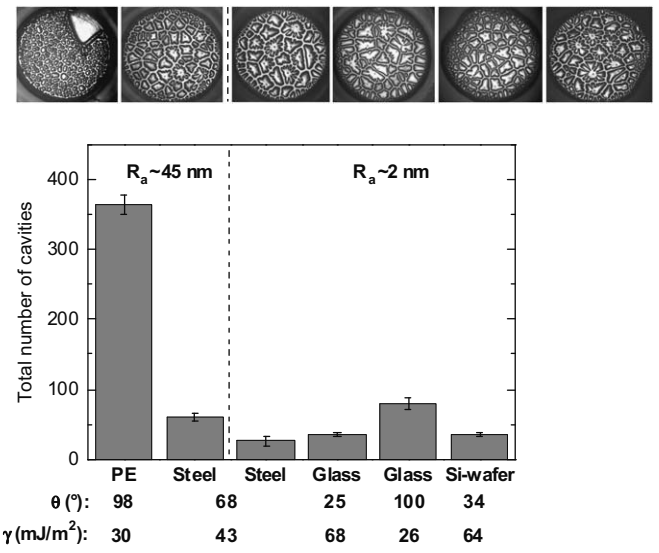

Fig. 2. Representative images of contact area for the probes of different materials obtained using BA/MA PSA ($M_w = 192{,}000$ g/mol) as PSA and total number of cavities calculated from these images. Contact angle probe/water and surface energy values are also given.

hydrophobic probes. The cavity growth rate for both types of cavities was also determined. Different growth modes were observed on the smooth and rough probe surface. The cavity growth rate is insensitive to the viscoelastic properties of the polymer (on the smooth probe), and decreases with increasing value of the G′ modulus (on the rough substrate).

3.2. Influence of the additional incorporated comonomer on the adhesion of BA/MA PSA

According to earlier studies [24,25], changes of the monomer composition often change both, the bulk and surface properties and, accordingly, the adhesion performance of PSA. Fig. 3 shows the shear moduli G′ and G″ as a function of frequency for acrylate copolymers with similar molecular weight, but different composition. The increasing in polarity of the incorporated comonomer (HEA→MMA→AA) leads to an increase in G′ and G″ of the copolymer. Incorporating of HEA practically does not change the rheological properties, while incorporating of AA changes the behavior of PSA to predominantly elastic (G′ > G″). Fig. 4 shows refractive index profiles of the near-surface region extracted from X-ray reflectivity data. The vertical lines mark the values of the refractive index of the statistical copolymer and the related homopolymers as shown by the labels and the depth $z=0$ denotes the sample surface. The composition of the PSA films near the surface differs from the composition in the bulk film. Fig. 4 shows the refractive index profiles for a distance from the sample surface between $0 < z < 400$ Å, in order to emphasize the near-surface composition. At $z > 400$ Å the compositions of the films in all cases converge to the average composition of the statistical copolymers. The surface of BA/MA copolymer is enriched with BA, while the surfaces of other copolymers are not enriched with BA. Although it is not possible to calculate the composition of a ternary system directly one can clearly see that the surface of BA/MA/AA film is enriched with AA. For BA/MA/HEA and BA/MA/MMA films, the results are ambiguous, we can conclude that in both cases the surface is not enriched with BA, and in the BA/MA/MMA film, there is an MA enriched region close to the surface. Our experiments also show that incorporation of the additional comonomer practically does not change the surface energy of the copolymer: γ(BA/MA)=32 ± 6 mJ/m^2, γ(BA/MA/HEA)=31 ± 5.9 mJ/m^2, γ(BA/MA/MMA)=32 ± 6.1 mJ/m^2 and γ(BA/MA/AA)=30 ± 6.1 mJ/m^2. Within experimental error all these values are equal. Lliterature values of the surface energies of the homopolymers are γ(PBA)=30.7 mJ/m^2, γ(PMA)=41 mJ/m^2, γ(PHEA)=37 mJ/m^2, γ(PMMA)=35 mJ/m^2 and γ(PAA)=30 mJ/m^2 [39,40]. Note, that the surface energy values of BA/MA and BA/MA/AA copolymers are close to surface energy values of PBA and PAA, respectively, presumably, since the surfaces are enriched with these homopolymers.

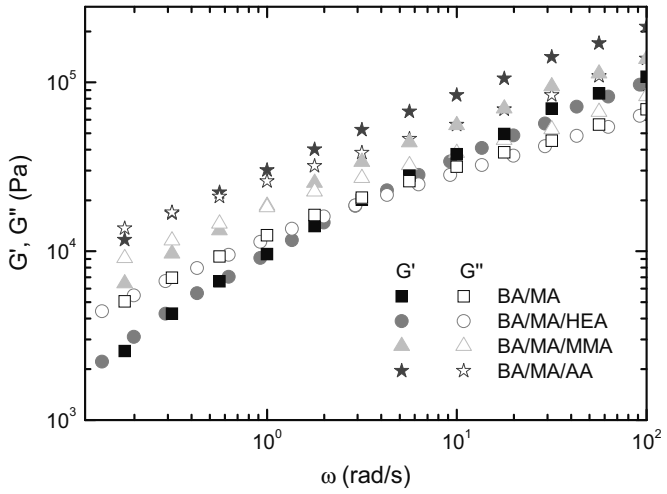

Fig. 3. Shear modulus (G′—storage modulus; G″—loss modulus) as a function of frequency for PSAs with different composition (M_w ~ 190,000 g/mol). Measurements are performed at room temperature.

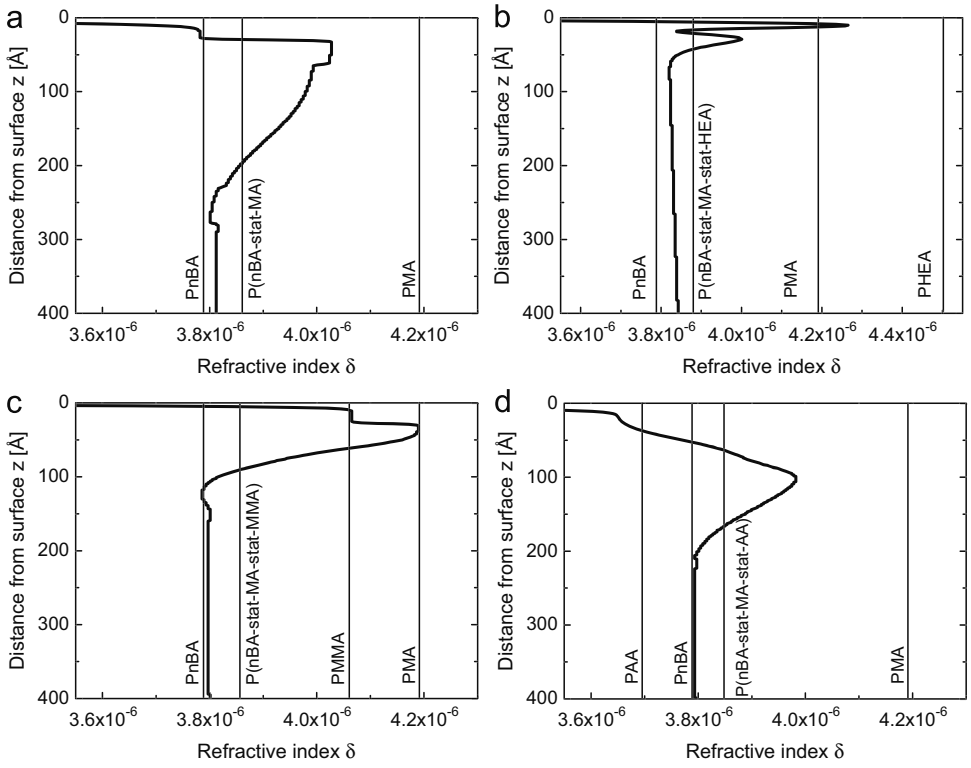

Fig. 4. Refractive index profiles of the near-surface region extracted from X-ray reflectivity data of BA/MA (a), BA/MA/HEA (b), BA/MA/MMA (c) and BA/MA/AA (d) films.

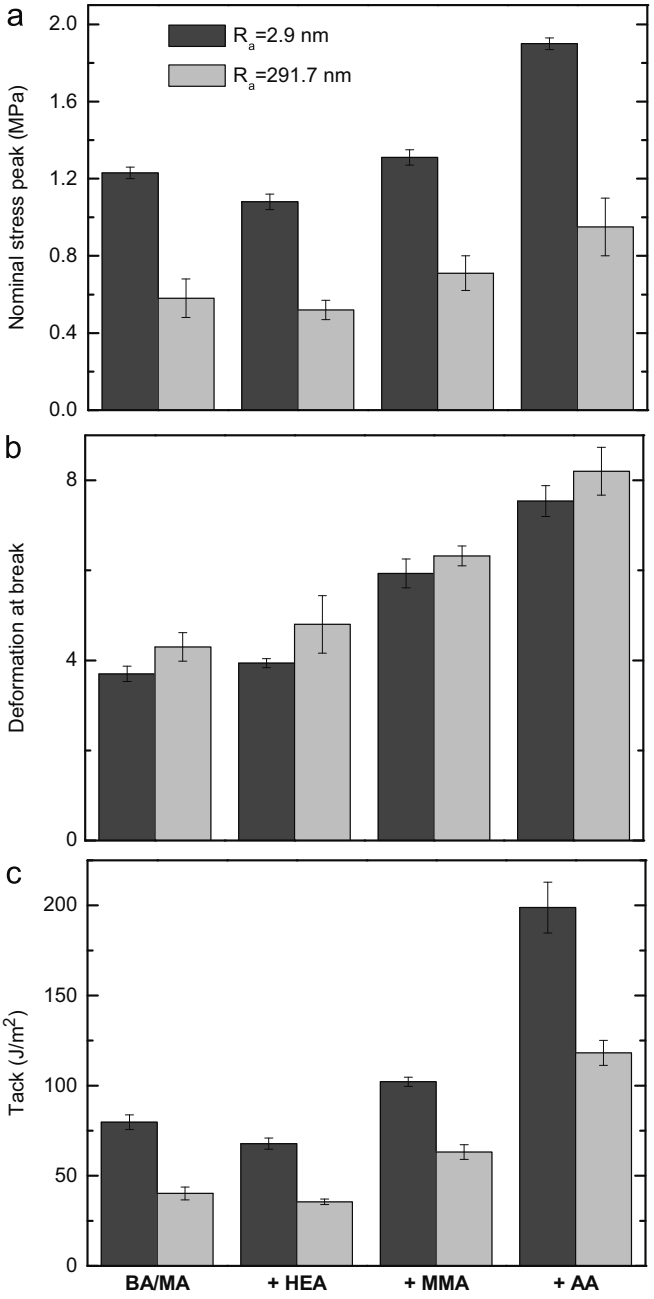

Fig. 5. Nominal stress peak (a), deformation at break (b) and tack (c) for PSAs with different composition (M_w~190,000 g/mol), calculated from stress–strain curves measured using the steel probes of R_a=2.9 and 291.7 nm.

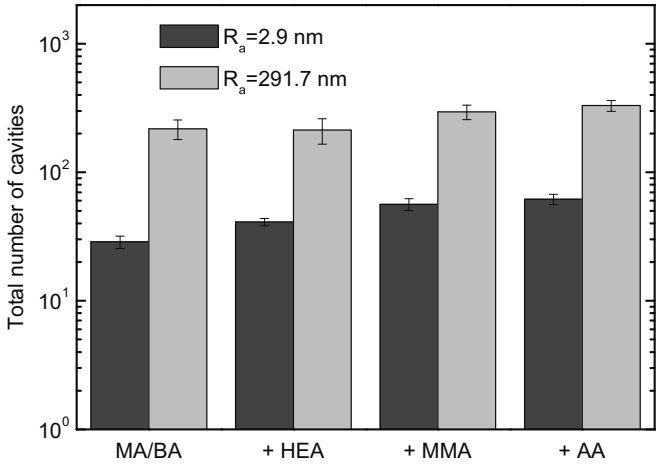

Fig. 6. Total number of cavities for PSAs with different composition (M_w~190,000 g/mol), measured using the steel probes of R_a=2.9 and 291.7 nm.

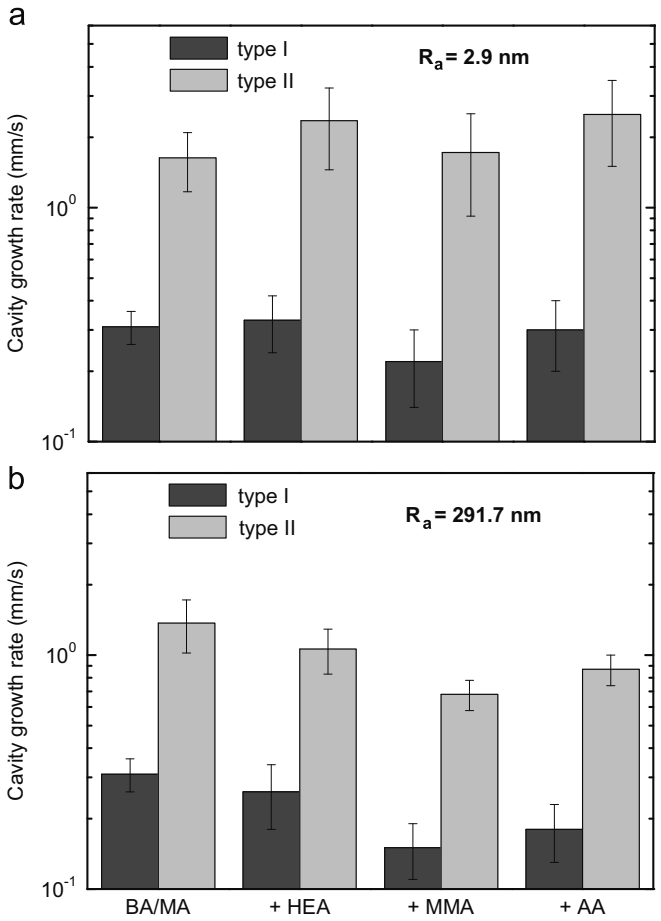

Fig. 7. Cavity growth rate for PSAs with different composition (M_w~190,000 g/mol) measured using the steel probes of R_a=2.9 nm (a) and 291.7 nm (b): type I cavities occurring at the beginning of debonding; type II cavities occuring in the area of the stress peak.

Fig. 5 shows the values of the parameters, calculated from stress–strain curves, i.e. stress peak, deformation at break and tack for PSAs with different composition. For our experiments we used two steel probes with various R_a. One can assume that in case of a rough probe, which goes deep into the PSA film during the tack test, the bulk properties of PSA play the decisive role in adhesion. In contrast, in case of a smooth probe the surface composition/properties are assumed to determine the adhesion behavior of PSA. Fig. 5 shows, that for both probes the values of stress peak, deformation at break and tack increase with increasing polarity of the incorporated comonomer, the copolymer containing AA has the highest values. However, the values of stress peak, deformation at break and tack also increase with increasing shear modulus. One can suppose that the viscoelastic properties of the PSA, especially on the rough surface, greatly influence its tack.

The total number of cavities as calculated from the images of the contact area of the probe with PSAs is shown in Fig. 6. The cavitation process is influenced by the polarity of incorporated comonomer: increasing comonomer polarity leads to an increase in the number of cavities. The PSA containing AA has the highest

number of cavities. It is worth noting, that in case of a smooth probe this effect is even more pronounced. This is attributed to a worse wetting of the probe in case of the AA containing copolymer, with its surface enriched with AA (Fig. 4). Thus experiments with both probes of different roughness demonstrate that worse wetting results in a larger number of cavities. But this is not only an interfacial effect related to the high polarity of the AA- enriched surface layer. Worse wetting is also due to an increased modulus for the PSA including AA. An additional consequence of the enhanced modulus is the high stress peak observed despite the poor wetting mentioned above. Thus, bulk properties play the decisive role in the adhesion.

Debonding of BA/MA PSAs with an additional incorporated comonomer is also accompanied by the appearance of two types of cavities [9]. Fig. 7 shows the cavity growth rates for copolymers of different composition. On the rough surface, the growth rate is determined by the viscoelastic properties of PSA, i.e. an increase in the modulus leads to a decrease in cavity growth rate. On the smooth surface, there is no dependence on the composition of copolymers and their viscoelastic properties; one can assume that in this case, the cavities grow on the surface and not in the bulk.

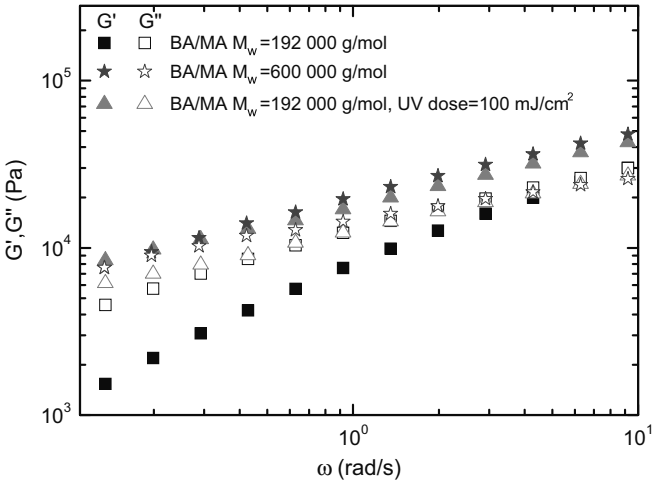

Fig. 8. Shear modulus (G′—storage modulus; G″—loss modulus) as a function of frequency for BA/MA PSAs (M_w=192,000 g/mol, M_w=600,000 g/mol and M_w=192,000 g/mol cured with UV dose=100 mJ/cm^2). Measurements are performed at room temperature.

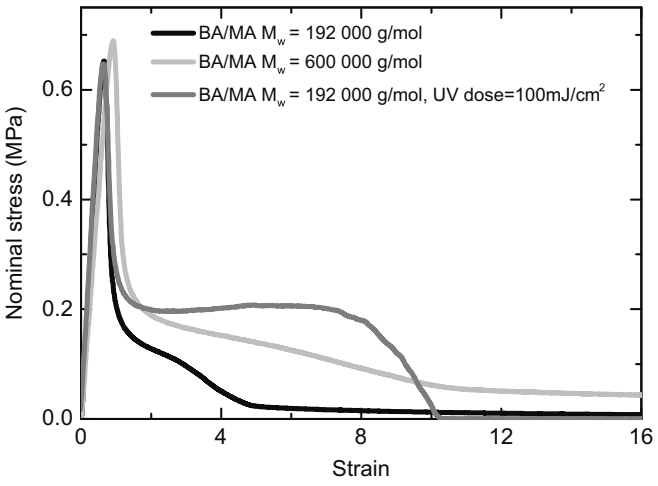

Fig. 9. Representative nominal stress–strain curves for BA/MA PSAs (M_w=192,000 g/mol, M_w=600,000 g/mol and M_w=192,000 g/mol cured with UV dose=100 mJ/cm^2) measured with steel probe of R_a=291.7 nm.

3.3. Cohesive vs. adhesive failure (crosslinking)

The systems discussed above are non-crosslinked copolymers and under the experimental conditions chosen for tack tests presented here the failure was always cohesive. The crosslinking of polymers changes not only their viscoelastic properties but can also change the mechanism of debonding. The adhesive properties of a BA/MA copolymer cured with various UV doses (0–100 mJ/cm^2) were

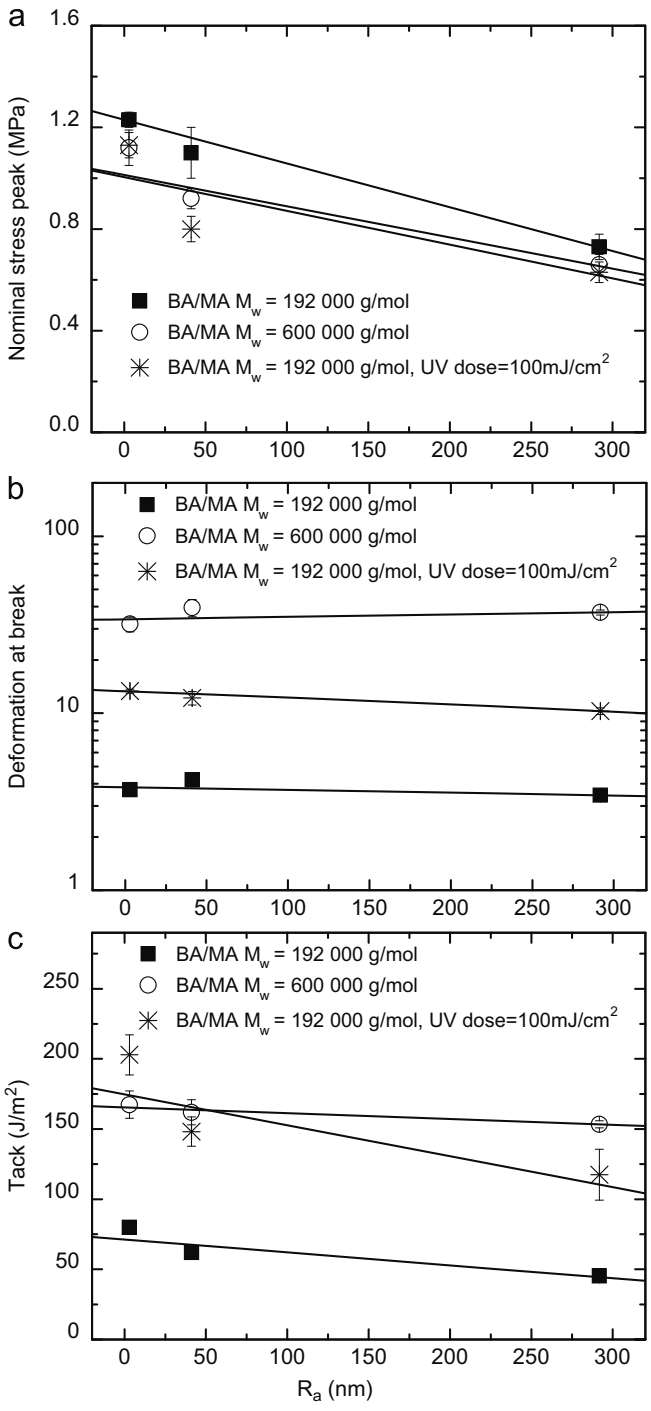

Fig. 10. Nominal stress peak (a), deformation at break (b) and tack (c) curves for BA/MA PSAs (M_w=192,000 g/mol, M_w=600,000 g/mol and M_w=192,000 g/mol cured with UV dose=100 mJ/cm^2) vs. R_a of the steel probe.

studied. Fig. 8 shows the shear moduli G′ and G″ as a function of frequency for BA/MA copolymers with M_w=192,000 and 600,000 g/mol, and for BA/MA copolymer with M_w=192,000 g/mol cured with a UV dose of 100 mJ/cm^2. Crosslinking leads to an increase of the shear modulus and the crosslinked BA/MA copolymer exhibits shear modulus magnitudes similar to the high molecular weight copolymer values. But in contrast to the non-crosslinked system no crossover of G′ and G″ is observed within the investigated frequency range. This indicates that the crosslinked polymer does not show a terminal flow regime or, at least, the longest relaxation time is much larger than for the uncrosslinked polymer with the higher molecular weight. Fig. 9 shows representative stress–strain curves measured with a steel probe of R_a=291.7 nm for uncrosslinked and crosslinked copolymers and Fig. 10 shows the dependence of the parameters, calculated from tack curves, i.e. stress peak, deformation at break and tack as a function of R_a for the same systems. In agreement with earlier studies, crosslinking shows very little effect on stress peak values, but strongly increases the stress plateau and the corresponding tack. The tack values for high molecular weight PSA are similar to the corresponding crosslinked one. Deformation at break increases with crosslinking, but does not reach the value of that for high molecular weight PSA. This is attributed to the different viscoelastic properties with respect to the terminal flow regime. Finally, it should be emphasized that the failure was cohesive in the case of the uncrosslinked copolymers, but adhesive in the case of crosslinked ones under the test conditions chosen here.

Images of the contact area of the probe with the PSA were recorded simultaneously with the tack curves. Fig. 11 shows the number of cavities and the stress as a function of time for uncrosslinked and crosslinked copolymers. The corresponding images are also given. The formation of the first cavities, in all cases, starts at time long before the stress reaches the maximum value. The number of cavities increases slowly at the beginning of debonding and then grows rapidly as the stress peak is approached. For the BA/MA film with M_w=192,000 g/mol new cavities do not appear after the stress peak is approached. We can also conclude that, for crosslinked copolymers the stress peak appear much earlier than for uncrosslinked ones, and in case of high molecular weight PSA and the crosslinked one additional cavities appear even after stress peak is passed. Nevertheless, the final number of cavities for the high molecular weight PSA and crosslinked PSAs is practically identical. Thus, cavitation is determined by the viscoelastic properties of the PSA regardless of the debonding mechanism (cohesive or adhesive failure).

Fig. 12 shows the cavity growth rate for different PSA systems on the steel probes with two different R_a. We compare uncrosslinked BA/MA with different molecular weights, crosslinked BA/MA and BA/MA/AA PSAs. It should be noted that the shear modulus increases with increasing M_w, with the degree of crosslinking and with the addition of AA. BA/MA/AA, crosslinked BA/MA with M_w= 192,000 g/mol and BA/MA with M_w=600,000 g/mol exhibit a similar shear modulus (see Figs. 3 and 8). On the smooth surface (Fig. 12a), there is no clear influence of PSA properties on the cavity growth rate, presumably the cavities grow on the surface. In contrast, on the rough surface (Fig. 12b), the cavity growth rate is controlled by the viscoelastic properties of PSA independent of the debonding mechanism (cohesive or adhesive failure), and it decreases significantly with increasing shear modulus. Therefore, we may conclude that, in case of the smooth probe cavities grow laterally along the probe surface (Fig. 12c), but they grow omnidirectionally into the polymer film for rough probes (Fig. 12d).

Lateral and vertical cavity growth have been observed in earlier studies [41,42]. In contrast to our investigation, the appearance of different mode of cavity expansion was not caused by the substrate roughness, but was provoked by the viscoelastic properties of the adhesive film. Leger and Creton [41] have analyzed, two different mechanisms of cavity growth of PSAs depending on the ration of the critical energy release rate G_c, which related to the interfacial structure, and the bulk elastic modulus E of the adhesive layer. If G_c/E is high cavities will grow in the bulk of the polymer, while low G_c/E values lead to interfacial propagation. Yamaguchi et al. [42] have investigated the height and width of the cavities as a function of time for 2-ethylhexylacrylate/ethyl acetate/acrylic acid tri-block and they detected that increasing the cross-linking density result in decrease in the cavity height, while the width increases. The authors conclude that the cavities in highly cross-linked samples expand laterally, rather than in the bulk of the polymer.

4. Concluding remarks

The adhesion behavior of statistical butyl acrylate-methyl acrylate copolymers has been investigated using the probe tack

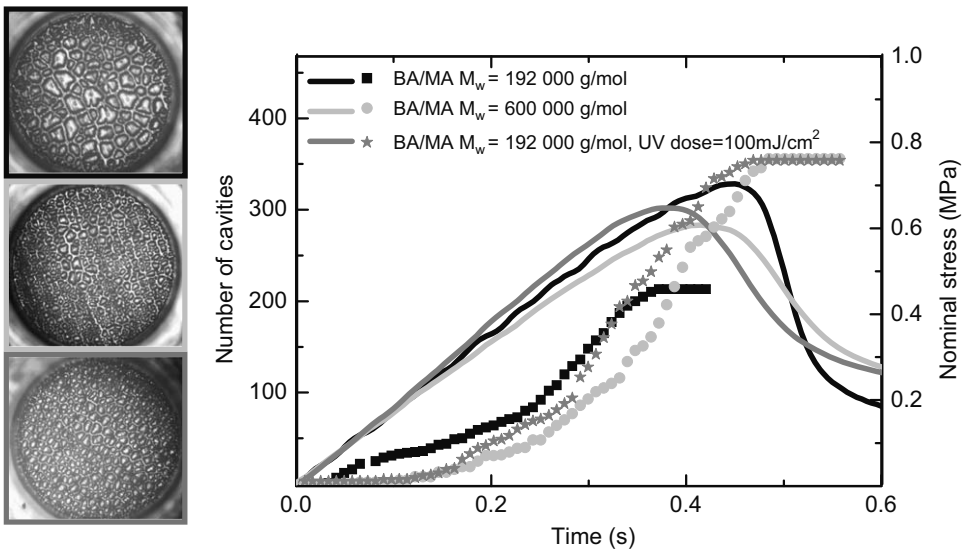

Fig. 11. Number of cavities (symbols) and nominal stress (lines) as functions of time for BA/MA PSAs (M_w=192,000 g/mol, M_w=600,000 g/mol and M_w=192,000 g/mol cured with UV dose=100 mJ/cm^2) measured with steel probe of R_a=291.7 nm. The corresponding images of contact area are also given.

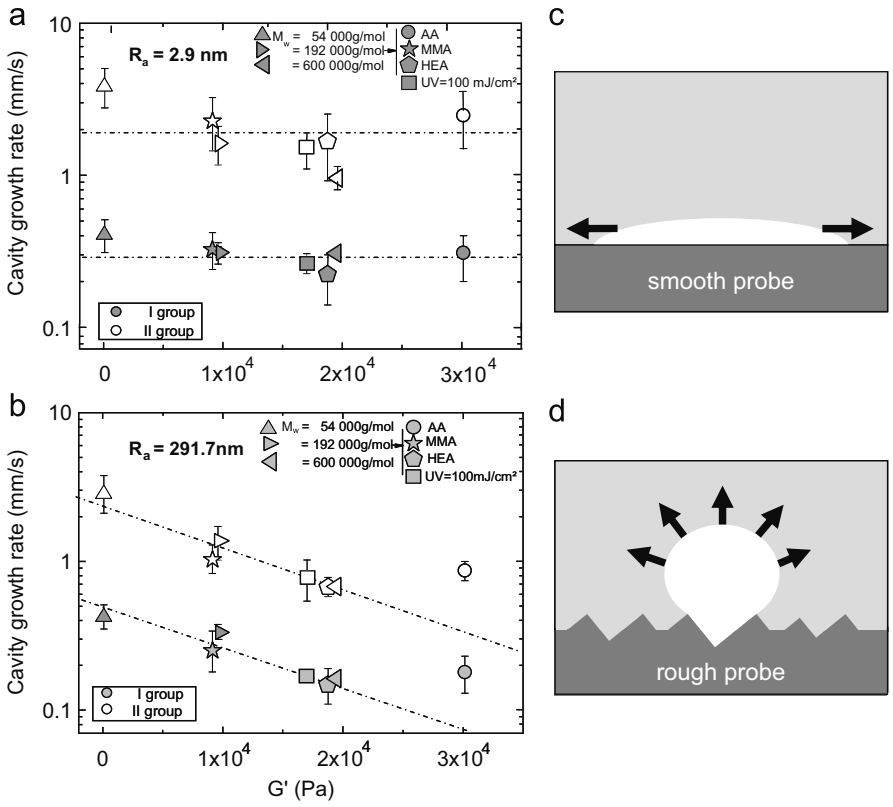

Fig. 12. Cavity growth rate for BA/MA PSAs (M_w=54,000 g/mol, M_w=192,000 g/mol, M_w=600,000 g/mol and M_w=192,000 g/mol cured with UV dose=100 mJ/cm^2) and for BA/MA/AA PSA measured using the steel probes of R_a=2.9 nm (a) and 291.7 nm (b). The corresponding schemes of the cavity growth on the smooth (c) and on the rough (d) surface are also given. The higher values of AA are due to the higher stress peak.

test in combination with video-optical imaging of the cavitation process. The effect of the substrate properties, incorporating of functional comonomer and crosslinking has been studied.

The stress peak and tack increase and the number of cavities decreases with increasing surface energy of the substrate. In particular, the latter indicates that this is due to better wetting.

The incorporation of an additional polar comonomer increases the shear modulus, stress peak, deformation at break and tack as well as the total number of cavities. The addition of a polar monomer does not effect the surface energy, as determined from contact angle measurements, but changes the near-surface composition in a non-trivial manner.

Crosslinking of BA/MA PSA results in an increase of the tack value. Crosslinked and high molecular weight BA/MA PSA show the best adhesion. Nevertheless, the change of the modulus seems to be the dominating factor, with respect to the observed changes in wetting and adhesion. Due to a higher stress peak level during fibril stretching, the mode of failure changes from cohesive to adhesive, but the cavitation process is not affected by crosslinking when samples with similar shear moduli are compared.

Independently of the bonding mechanism (cohesive or adhesive failure) in case of a rough probe, the cavity growth rate significantly decrease with increasing shear modulus of PSA, in case of a smooth probe, this characteristic quantity is insensitive to the viscoelastic properties of the PSA. Comparing the cavitation process for uncrosslinked BA/MA with different M_w, crosslinked BA/MA and also the BA/MA polymer including various polar comonomers reveals, that the cavity growth rate decreases with increasing modulus on the rough substrate, but is independent of the modulus on the smooth substrate. Therefore, we postulate two different modes of cavity growth: lateral growth along the interface on the smooth substrate and omnidirectional growth into the polymer film on the rough substrate.

Acknowledgments

Financial support by the Deutsche Forschungsgemeinschaft (DFG) under grant numbers WI 3138/2 and MU1487/6 is gratefully acknowledged. We thank Dr. U. Licht (BASF) for providing of the model copolymers. We also thank D. Paul for invaluable help with upgrading the Texture Analyzer, A. Reif for polishing the probes, Dr. Svetlana Guriyanova for support by SPM measurements, A. Kienzler for characterization of the probes using white light confocal microscope NanoFocus µSurf® and Prof. S. Neser for adapting the features of Visiometrics Image Processing System software.

References

[1] Benedek I, Feldstein MM, editors. Handbook of pressure-sensitive adhesives and products; vol. 1: fundamentals of pressure-sensitivity; vol. 2: technology of pressure-sensitive adhesives and products; vol. 3: applications of pressure-sensitive products. Boca Raton, London, New York: CRC—Taylor & Francis; 2009.
[2] Creton C, Fabre P. Tack. In: Dillard DA, Pocius AV, editors. Adhesion science and engineering; vol. 1: the mechanics of adhesion. Amsterdam: Elsevier; 2002. p. 535–76.
[3] Zosel A. Adhesion and tack of polymers: influence of mechanical properties and surface tensions. Colloid Polym Sci 1985;263:541–53.
[4] Creton C, Leibler L. How does tack depend on time of contact and contact pressure? J Polym Sci Part B: Polym Phys 1996;34:545–54.
[5] Tordjeman P, Papon E, Villenave JJ. Tack properties of pressure-sensitive adhesives. J Polym Sci Part B: Polym Phys 2000;38:1201–8.

[6] Hooker J, Creton C, Shull KR, Tordjeman P. Surface effects on the microscopic adhesion mechanisms of SIS+resin PSA's. In: Proceedings of the 22nd annual meeting of the adhesion society. Panama City Beach, USA; 1999.
[7] Chiche A, Pareige P, Creton C. Role of surface roughness in controlling the adhesion of a soft adhesive on a hard surface. C R Phys 2000;1:1197–204.
[8] Chiche A, Dollhofer J, Creton C. Cavity growth in soft adhesives. Eur Phys J E: Soft Matter Biol Phys 2005;17:389–401.
[9] Peykova Y, Guriyanova S, Lebedeva OV, Diethert A, Müller-Buschbaum P, Willenbacher N. The effect of surface roughness on adhesive properties of acrylic copolymers. Int J Adhes Adhes 2010;30:245–54.
[10] Toyama M, Ito T, Moriguchi H. Studies on tack of pressure-sensitive adhesive tapes. J Appl Polym Sci 1970;14:2039–48.
[11] Toyama M, Ito T, Nukatsuka H, Ikeda M. Studies on tack of pressure-sensitive adhesive tapes: on the relationship between pressure-sensitive adhesion and surface energy of adherends. J Appl Polym Sci 1973;17:3495–502.
[12] Creton C, Hooker J, Shull KR. Bulk and interfacial contributions to the debonding mechanisms of soft adhesives: extension to large strains. Langmuir 2001;17:4948–54.
[13] Agirre A, Nase J, Creton C, Asua JM. Adhesives for low-energy surfaces. Macromol Symp 2009;281:181–90.
[14] Jovanovic R, Dube MA. Screening experiments for butyl acrylate/vinyl acetate pressure-sensitive adhesives. Ind Eng Chem Res 2005;44:6668–75.
[15] Carelli C, Deplace F, Boissonnet L, Creton C. Effect of a gradient in viscoelastic properties on the debonding mechanisms of soft adhesives. J Adhes 2007;83: 491–505.
[16] Deplace F, Carelli C, Mariot S, Retsos H, Chateauminois A, Ouzineb K, et al. Fine tuning the adhesive properties of a soft nanostructured adhesive with rheological measurements. J Adhes 2009;85:18–54.
[17] Deplace F, Rabjohns MA, Yamaguchi T, Foster AB, Carelli C, Lei CH, et al. Deformation and adhesion of a periodic soft–soft nanocomposite designed with structured polymer colloid particles. Soft Matter 2009;5:1440–7.
[18] Krenceski MA, Johnson JF. Shear, tack and peel of polyisobutylene: effect of molecular weight and molecular weight distribution. Polym Eng Sci 1989;29: 36–43.
[19] Zosel A. Fracture energy and tack of pressure sensitive adhesives. In: Satas D, editor. Advances in pressure sensitive adhesives technology, vol. 1. Warwick, RI: Satas & Associates; 1992. p. 92–127.
[20] Lakrout H, Creton C, Ahn D, Shull KR. Influence of molecular features on the tackiness of acrylic polymer melts. Macromolecules 2001;34:7448–58.
[21] O'Connor AE, Willenbacher N. The effect of molecular weight and temperature on tack properties of model polyisobutylenes. Int J Adhes Adhes 2004;24:335–46.
[22] Gower MD, Shanks RA. The effect of varied monomer composition on adhesive performance and peeling master curves for acrylic pressure-sensitive adhesives. J Appl Polym Sci 2004;93:2909–17.
[23] Gower MD, Shanks RA. Comparison of styrene with methyl methacrylate copolymers on the adhesive performance and peeling master curves of acrylate pressure sensitive adhesives. Macromol Chem Phys 2005;206: 1015–27.
[24] Aubrey DW, Ginosatis S. Peel adhesion behavior of carboxylic elastomers. J Adhes 1981;12:189–98.
[25] Chan HK, Howard GJ. Structure-property relationships in acrylic adhesives. J Adhes 1978;9:279–304.
[26] Ahn D, Shull KR. Effects of methylation and neutralization of carboxylated poly(*n*-butyl acrylate) on the interfacial and bulk contributions to adhesion. Langmuir 1998;14:3637–45.
[27] Lindner A, Lestriez B, Mariot S, Creton C, Maevis T, Luhmann B, et al. Adhesive and rheological properties of lightly crosslinked model acrylic networks. J Adhes 2006;82:267–310.
[28] Zosel A, Barwich J. Mechanical properties and adhesion performance of UV crosslincable hot melt pressure sensitive adhesives. PSTC Pressure Sensitive Adhesive Tape. In: Conference proceedings Orlando 3rd–5th May 1995. p. 175–87.
[29] Czech Z. Synthesis and cross-linking of acrylic PSA systems. J Adhes Sci Technol 2007;21:625–35.
[30] Zosel A. Effect of cross-linking on tack and peel strength of polymers. J Adhes 1991;34:201–9.
[31] Zosel A. The effect of fibrilation on the tack of pressure sensitive adhesives. Int J Adhes Adhes 1998;18:265–71.
[32] Do HS, Park YJ, Kim HJ. Preparation and adhesion performance of UV-crosslinkable acrylic pressure sensitive adhesives. J Adhes Sci Technol 2006;20:1529–45.
[33] Wu GL, Jiang Y, Ye L, Zeng SJ, Yu PR, Xu WJ. A novel UV-crosslinked pressure-sensitive adhesive based on photoinitiator-grafted SBS. Int J Adhes Adhes 2010;30:43–6.
[34] Parratt LG. Surface studies of solids by total reflection of X-rays. Phys Rev 1954;95:359–69.
[35] Diethert A, Peykova Y, Willenbacher N, Muller-Buschbaum P. Near-surface composition profiles and the adhesive properties of statistical copolymer films being model systems of pressure sensitive adhesive films. ACS Appl Mater Interfaces 2010;2:2060–8.
[36] Fuji M, Fujimori H, Takei T, Watanabe T, Chikazawa M. Wettability of glass-bead surface modified by trimethylchlorosilane. J Phys Chem B 1998;102:10498–504.
[37] Forny L, Pezron I, Saleh K, Guigon P, Komunjer L. Peculiar absorption of water by hydrophobized glass beads. Colloids Surf A 2005;270–271:263–9.
[38] Owens DK, Wendt RC. Estimation of the surface free energy of polymers. J Appl Polym Sci 1969;13:1741–7.
[39] Brandrup J, Immergut EH, Grulke EA, editors. Solid state properties. 4th edition: VI. John Wiley & Sons; 1999.
[40] Friedsam C, Del Campo Becares A, Jonas U, Seitz M, Gaub HE. Adsorption of polyacrylic acid on self-assembled monolayers investigated by single-molecule force spectroscopy. New J Phys 2004;6:9.
[41] Leger L, Creton C. Adhesion mechanisms at soft polymer interfaces. Philos Trans R Soc A 2008;366:1425–42.
[42] Yamaguchi T, Koike K, Doi M. In situ observation of stereoscopic shapes of cavities in soft adhesives. Europhys Lett 2007;77:64002.